MASTER COPY   -   FOR REPRODUCTION PURPOSES

SECURITY CLASSIFICATION OF THIS PAGE (When Data Entered)

AD-A191 451

REPORT DOCUMENTATION PAGE	READ INSTRUCTIONS BEFORE COMPLETING FORM	
1. REPORT NUMBER ARO 24165.4-MS	2. GOVT ACCESSION NO. N/A	3. RECIPIENT'S CATALOG NUMBER N/A
4. TITLE (and Subtitle) Preferential Surface Adsorption in Miscible Blends of Polystyrene and Poly(vinyl methyl ether)	5. TYPE OF REPORT & PERIOD COVERED Technical	
	6. PERFORMING ORG. REPORT NUMBER	
7. AUTHOR(s) Q. S. Bhatia, D. H. Pan, and J. T. Koberstein	8. CONTRACT OR GRANT NUMBER(s) DAAL03-86-K-0133	
9. PERFORMING ORGANIZATION NAME AND ADDRESS University of Connecticut Storrs, CT 06268	10. PROGRAM ELEMENT, PROJECT, TASK AREA & WORK UNIT NUMBERS	
11. CONTROLLING OFFICE NAME AND ADDRESS U. S. Army Research Office Post Office Box 12211 Research Triangle Park, NC 27709	12. REPORT DATE Feb. 2, 1988	
	13. NUMBER OF PAGES 43	
14. MONITORING AGENCY NAME & ADDRESS(if different from Controlling Office)	15. SECURITY CLASS. (of this report) Unclassified	
	15a. DECLASSIFICATION/DOWNGRADING SCHEDULE	

16. DISTRIBUTION STATEMENT (of this Report)

Approved for public release; distribution unlimited.

17. DISTRIBUTION STATEMENT (of the abstract entered in Block 20, if different from Report)

NA

18. SUPPLEMENTARY NOTES   (accepted for Macromolecules)
The view, opinions, and/or findings contained in this report are
those of the author(s) and should not be construed as an official
Department of the Army position, policy, or decision, unless so
designated by other documentation.

19. KEY WORDS (Continue on reverse side if necessary and identify by block number)
Miscible polymer blends; x-ray photoelectron spectroscopy, Surface
Adsorption; surface tension; polystyrene; poly(vinyl methyl ether)

20. ABSTRACT (Continue on reverse side if necessary and identify by block number)

see attached

DD FORM 1473   EDITION OF 1 NOV 65 IS OBSOLETE

UNCLASSIFIED

SECURITY CLASSIFICATION OF THIS PAGE (When Data Entered)

Preferential Surface Adsorption in Miscible

Blends of Polystyrene and Poly(vinyl Methyl ether)

Technical Report No. 4

-

Q. S. Bhatia, D. H. Pan, and J. T. Koberstein
(accepted for Macromolecules)

February 1988

88

Preferential Surface Adsorption in Miscible

Blends of Polystyrene and Poly(vinyl methyl ether)

Qamardeep S. Bhatia
Department of Chemical Engineering
Princeton University
Princeton, NJ 08544

David H. Pan
Xerox Webster Research Center
800 Phillips Road 0114/39D
Webster, NY 14580

and

Jeffrey T. Koberstein*
Institute of Materials Science and
Department of Chemical Engineering
University of Connecticut
Storrs, CT 06268

*to whom correspondence should be addressed.

ABSTRACT

The surface structure and properties of miscible blends of polystyrene (PS) with poly(vinyl methyl ether) (PVME) have been studied as a function of the blend composition and constituent molecular weights. The lower surface tension of hte PVME compared to that of PS results in preferential adsorption of PVME at the surface. The surface PVME enrichment is characterized by measurements of the surface tension as a function of the temperature, accomplished with an automated pendant drop apparatus, and by x-ray photoelecron spectroscopy (XPS). Angle-dependent XPS has been used to determine the surface concentraiton profiles of the blend constituents. The results of these measurements demonstrate that: 1) the PVME surface concentration is elevated substantially from that in the bulk; 2) the integrated surface concentration gradient detemrined from XPS measurements can be modeled as a $\coth^2(z/\xi+\alpha)$ profile where ξ is the screening length; and 3) the degree of surface enrichment depends strongly on the blend composition and molecular weight of the constituents, correlating well with the surface energy difference between PS and PVME.

I. __INTRODUCTION__

Current technologies frequently employ multiconstituent polymer systems in order to tailor the material's bulk physical and mechanical properties. Although much emphasis has been placed on understanding the bulk phase relationships and properties of multicomponent polymeric materials, comparitively little is known about their surface structure and properties.

In small molecule systems, such as metallic alloys[1] and liquid mixtures[2], it is well known that the surface composition differs from that of the bulk due to preferential surface adsorption of one constituent. This process is driven, in part, by differences in surface energies and can be expressed classically through the Gibbs adsorption isotherm[3]

$$-d\gamma = \Sigma_i \; \Gamma_i \; d\mu_i \qquad\qquad (1)$$

where Γ_i is the surface excess ($\Gamma_i \equiv n_i/A$) of component i, dA the fractional surface area, and μ_i is the chemical potential of species i for n_i moles of that component. From (1) it is apparent that a surface concentration gradient exists in multiconstituent systems where the surface is enriched in the component of lower surface energy (i.e., surface tension γ).

Preferential surface adsorption has been documented by surface tension, contact angle and x-ray photoelectron spectroscopy (XPS) measurements on several multicomponent polymeric systems. In immiscible binary homopolymer blends, for example, the surface behavior is generally dominated by adsorption of the lower surface energy component.[4,5] This phenomena also occurs for many blend additives.[6] Since equilibrium bulk thermodynamics favor complete demixing of the two homopolymers, the "equilibrium" surface should be occupied exclusively by the constituent of lower surface energy. In actuality, macroscopic

equlibrium is usually not attained in immiscible polymer blends, such that the surface structure obtained is dependent on intrinsic factors such as the relative wettabilities of the two constituents and the degree of phase separation; as well as extrinsic factors including the procedure for sample preparation and blend morphology.

A number of investigations of copolymer surfaces have also appeared. Early studies of the surface tensions of block copolymer melts[7,8] illustrated significant surface activity by the sequence of lower surface energy. Surface activity increased with block length, and complete surface coverage by the low surface energy constituent was observed for copolymers of sufficient length. XPS investigations have reported similar results for a number of diblock and triblock copolymer systems.[9-15] Surface enrichment has also been demonstrated in random copolymers of hexamethyl sebacate with dimethyl siloxane and ethylene oxide with propylene oxide.[7] Complete domination of the surface by lower energy constituent does not occur however, reflecting the influence of configurational constraints which limit migration to the surface.

Block copolymers exhibit similar behavior when added to homopolymers.[16-18] A practical example is the reduction of poly(propylene glycol) surface tension in the manufacture of polyurethane foams.[19] The addition of a few tenths of a percent of certain polyether-polysiloxane block copolymers reduces the surface tension of the blend to that corresponding to pure polysiloxane.

The surface topology of block copolymers has also been investigated by XPS measurements. The results for a number of block copolymers containing dimethyl siloxane (PDMS) sequences[9,13] showed that the surface is comprised of a homogeneous PDMS-rich overlayer, the composition and thickness of which are dependent on the composition and block lengths of the copolymer. Under certain conditions, this overlayer consisted of essentially pure PDMS. In contrast, similar

studies on other block copolymer systems have concluded that, although the surface is dominated by the species of lower surface energy, the topology is heterogeneous.[10-12,14,15] That is, the species dominating the surface resided in either lens-shaped, cylindrical, or lamellar microdomains protruding from the surface.

Gaines[20] has attributed the two types of behavior observed for block copolymers to differences in spreading or wetting for the two systems. In the siloxane systems, the surface tension difference between components is large enough to favor surface wetting by the siloxane sequences. In cases where the surface energy difference is small, one sequence cannot wet the other, resulting in a heterogeneous surface as has been found in ethylene oxide block copolymers.[10,11]

More recently, Fredrickson[21] has proposed a theory for surface ordering in block copolymers. Even in the disordered state, block copolymers are shown to possess ordered surfaces with periodic surface composition profiles. The initial theory is derived for systems close to the order-disorder transition (i.e., in the weak segregation limit) and does not consider directly the effects associated with preferential wetting.

There is a large body of experimental data and theory pertaining to the surface properties of polymer solutions, especially concerning their surface tensions.[22-26] The success of these theories in representing the experimental data has been discussed in a recent review.[27] Most polymer-solvent systems show adsorptive behavior for the solute wherein a large initial reduction in surface tension (3-5 mN/m) is seen upon polymer addition. Repulsive behavior (i.e., surface enrichment of solvent) has also been observed for several polymer systems. In this case the surface tension increases almost linearly with polymer

concentration until it jumps suddenly to the pure homopolymer value as the polymer concentration approaches unity.

Miscible homopolymer blends are similar to polymer solutions and also exhibit pronounced surface-excess behavior.[7,28,29] Measurements on several oligomeric mixtures reveal that the surface excess is accentuated by increasing the molecular weight. LeGrand and Gaines[29] modelled the surface tension data for compatible oligomers of PDMS and polyisobutylene by a theory which combined the Flory-Huggins lattice model for polymer solutions[30] with the Prigogine-Marechal parallel-layer model.[2] In general, however, careful examination of theories for the surface tensions of miscible blends has been hampered by the lack of knowledge regarding the polymer-polymer interaction parameters.

Recently, Pan and Prest,[31] presented initial results of studies on the surface structure of the miscible polymer blend system polystyrene/poly(vinyl methyl ether). X-ray photoelectron spectroscopy were employed to measure both the effective surface composition and surface concentration gradient in the blends. The results demonstrated a pronounced surface enrichment of the poly(vinyl methyl ether). The bulk thermodynamic phase relationships, interaction parameters, and phase separation mechanisms have already been studied extensively for this miscible blend system.[32-37] The observed phase diagrams exhibit a lower critical solution temperature wherein phase separation occurs upon heating. Miscibility is manifest over a wide range of experimental conditions, making this blend an excellent model system for the study of preferential surface adsorption in polymer systems. In this communication, we extend the initial study and report the effects of blend composition and constituent molecular weights on surface enrichment in these miscible polymer blends. The surface structure is characterized by XPS measurements on thin films, while the thermodynamic character of the surface is assessed by determining the

surface tensions of blends in the melt state. The results obtained are compared to the predictions of various theories for the surface thermodynamics and structure of polymer solutions.

II. EXPERIMENTAL

A. Materials and Specimen Preparation

The molecular weights and molecular weight distributions (quoted from the suppliers) of the polystyrene and poly(vinyl methyl ether) specimens are reported in Table I. Prior to usage, the PVME was cleaned by precipitation from toluene solution by the addition of hexane. This procedure was repeated twice and was followed by vacuum drying at 60°C for a minimum of one week.

Blends containing 5, 20, 50 and 80% by weight of PVME, with the remainder consisting of one of the polystyrenes, were prepared by spin coating a 2% w/w solution of the blend in toluene onto aluminum substrates spun at 1000 rpm for 40 seconds. The spin coated specimens were dried on the substrates for two days in vacuum and were subsequently annealed for two weeks at temperatures in the range of 50-80°C, depending on the composition. Specimens for pendant drop measurements of surface tension were prepared by dissolving the blended materials in toluene and drying under vacuum for one week at 80°C.

B. Surface Tension Measurements

Surface tensions of the homopolymers and blends were evaluated as a function of blend composition and temperature using a pendant drop technique. The apparatus is shown schematically in Figure 1.

Drops of the blends and homopolymers were formed at elevated

Table I

Characteristics of Specimens

Sample Designation	M_w	M_w/M_n	Source*
PS1 (polystyrene)	517	< 1.06	3
PS2 (polystyrene)	1,200	< 1.06	1
PS3 (polystyrene)	2,100	< 1.10	2
PS4 (polystyrene)	3,100	< 1.06	1
PS5 (polystyrene)	4,000	< 1.10	2
PS6 (polystyrene)	9,000	< 1.04	2
PS7 (polystyrene)	20,400	< 1.06	2
PS8 (polystyrene)	50,000	< 1.06	2
PS9 (polystyrene)	110,000	< 1.06	2
PS10 (polystyrene)	127,000	< 1.06	1
PVME - poly(vinyl methyl ether)	99,000	~ 2.1	3

*1 = Polymer Laboratories
*2 = Pressure Chemical Company
*3 = Scientific Polymer Product

temperatures (ca. 100-170oC) using a Drummond positive displacement syringe with a glass capillary tip. Drops were formed inside a quartz cuvette which was placed in a Rame-Hart environmental chamber equipped with provisions for temperature control ($\pm$ 1oC). All measurements were carried out under argon atmosphere. The optical system consisted of a Questar M1 microscope coupled to an NEC T1-22A CCD camera. The optics were focussed by optimizing the video image of a reticle containing a finely ruled grid that was placed at the drop location. The reticle also provided a direct calibration of both the vertical and horizontal magnification factors inherent to the optics and camera system. The signal from the video camera was fed to a Tecmar Video Van Gogh Board which performed the frame grabbing and image digitization. Drop shape analysis was accomplished with a robust shape analysis algorithm.[40]

Estimation of the surface tension by the pendant drop technique requires a knowledge of the material density or specific volume. The specific volume relationship for PS4 (MW = 3100) was obtained by interpolation of the data of Bender and Gaines.[41] The resultant temperature dependent specific volume for PS4 is

$$v[cm^3/g] = 0.9310 + 6.0 \times 10^{-4} T[oC]. \tag{2}$$

A similar relationship for PVME was taken as[42]

$$v_{PVME} [cm^3/g] = 0.9709 + 5.92 \times 10^{-4} (T[oC]-25). \tag{3}$$

Blend densities were calculated from these expressions by assuming no volume change upon mixing. The densities of PS/PVME blends do exhibit a small positive deviation from additivity.[43] The constant volume assumption therefore yields a

density which is in error by approximately 1-2 percent. The precision in the surface tension measurements is $\pm$ 0.5 dyn/cm.

C.   XPS Instrumentation

XPS spectra were recorded with a modified AEI (Kratos) ES200B photoelectron spectrometer fitted with a Physical Electronics 04-151 achromatic $AlK_{\alpha 12}$ source ($h\nu$ = 1486.7 eV). Typical operating conditions were: X-ray source 10 KV, 60 mA, pressure in the source chamber 2-4 x 10^{-8} torr, and pressure in the analyzer chamber 6 x 10^{-7} torr. The electron energy analyzer was operated by a PDP 11/23 computer in the fixed retarding ratio mode (for molecular weight studies) or fixed analyzer transmission mode (for angle-dependent experiments) through four 18-bit digital-to-analog converters (Analog Devices) and a data acquisition software package. The typical number of scans for each spectrum was 4 to 8. Under the experimental conditions employed, the $Ag_{3d\ 5/2}$ peak at 386.27 eV binding energy had a full width at half maximum (FWHM) of 1.15 eV. Both PS and PVME contain hydrogen carbon and therefore the binding energy of the C_{1s} signal at 285.0 eV was used as an internal calibration of the absolute binding energy scale.

Angular-dependent XPS measurements were carried out by rotating the samples relative to the fixed analyzer position by an angle θ, designated as the take-off angle between the sample normal and the entrance slit in the analyzer. The effective sampling depth is decreased by increasing the electron takeoff angle.

III. ANALYSIS AND RESULTS

A.   Surface Tension

Surface tensions of miscible blends of PS and PVME, and the parent homopolymers were determined by digital image analysis of axisymmetric pendant fluid drops. A typical drop image is shown in Fig. 2a. The theoretical profile of the drop is governed by a balance between gravitational forces and surface tension as expressed by the dimensionless Bashforth-Adams equations[44]

$$d\phi/dS = 2/\beta + Z \, (\sin\phi)/X$$

$$dX/dS = \cos\phi$$

$$dZ/dS = \sin\phi \tag{4}$$

with boundary conditions

$$X(0) = 0, \, Z(0) = 0, \, d\phi/dS = 1/\beta, \, \phi(0) = 0. \tag{5}$$

The dimensionless spatial coordinates are defined as $X \equiv x\sqrt{c}$, $Z \equiv z\sqrt{c}$, where x and z are the real cartesion coordinates defining the drop profile, and $\sqrt{c}$ is the scale or magnification factor defined as

$$\sqrt{c} = \Delta\rho g/\gamma. \tag{6}$$

The density difference across the interface is $\Delta\rho$; g is the gravitational constant, and γ is the surface tension. The dimensionless shape factor is taken as $\beta = b\sqrt{c}$ while the dimensionless arc length is defined as $S = s\sqrt{c}$, where b and s are the radius of curvature at the drop apex and the arc length, respectively. The relationship of these variables and the angle ϕ to the drop profile are illustrated in Fig. 3.

The regression of the theoretical profile upon the experimental profile involves an optimization in five variables: x and z translations; a rotation of the camera axis with respect to the gravitational field; a magnification factor, $\sqrt{c}$; and the shape parameter β. This regression was performed using a robust shape

comparison algorithm.[40] The result of edge detection by global thresholding is illustrated in Figure 2b. The final comparison of this experimental profile with the theoretical profile resulting from solution of Eqns. (4-6) is shown in Fig. 2c. Details pertaining to the shape analysis are given elsewhere.[40]

The pendant drop technique has been used to determine the composition and temperature dependence of the surface tension for binary miscible blends of PVME (MW = 99,000) and PS4 (MW = 3100). The results are presented in Figures 4 and 5. The surface tensions of the blends are effectively linear in temperature (Fig. 4), as has been observed for pure homopolymers,[6] and show a temperature coefficient of $d\gamma/dT \sim -0.075$ dyn/cm/K.

The composition series (Fig. 5) demonstrates that there is a considerable surface excess of PVME in the blends. This is particularly notable in the 50/50 w/w blend where the observed surface tensions correspond closely to the values for pure PVME homopolymer. The driving force for preferential surface adsorption of PVME is its lower surface tension (21.9 dynes/cm @ 150°C) compared to that of PS4 (29.7 dynes/cm @ 150°C).

If the surface tension of the blend is assumed to be proportional to the fractional surface coverage of each constituent, the surface fraction PVME can be estimated as

$$f_{PVME} = (\gamma_{BLEND} - \gamma_{PS})/(\gamma_{PVME} - \gamma_{PS}). \tag{7}$$

It follows that the weight fraction of PVME at the surface is

$$\omega_{PVME} = f_{PVME}\,\rho_{PVME} / [f_{PVME}\,\rho_{PVME} + (1 - f_{PVME})\,\rho_{PS}] \tag{8}$$

where the densities are given by (2) and (3). The relative enrichment can be described through a distribution coefficient for PVME defined as

$$K_{PVME} = (\omega_S/\omega_B)_{PVME} \qquad (9)$$

where ω_S and ω_B are the surface and bulk weight fractions of PVME respectively. The results of these calculations (Table II) indicate strong adsorption of PVME at the surface. These data show clearly that the relative enrichment is inversely related to the bulk PVME content.

The surface tension behavior of polymer solutions has been the subject of extensive theoretical treatment. Particular approaches that have formed the bases of much of this effort are the parallel-layer model developed by Prigogine and coworkers[3] and extended to polymers by Gaines[22] et al., and the generalized square gradient theory popularized by Cahn[45] and adopted in many subsequent studies.[25,26,46]

For the case of surface tensions of polymers in solution with an attractive surface (i.e., the polymer is preferentially adsorbed at the air-solution interface) both approaches lead to an expression of the form

$$\gamma - \gamma_o = K_1 + K_2 \, \phi_b{}^m \qquad (10)$$

where γ_o is the surface tension of pure solvent, and ϕ_b is the bulk volume fraction of polymer in the solution. The constants K_1 and K_2 are dependent upon the local solute-interface interaction energy per unit surface area. The mean field theories[25,26] yield a prediction of $m = 1$, while the monolayer theory prediction is variable depending on the relative size of the constituents and the interaction

Table II

Surface Compositions from Surface Tension Data (150ºC)

Weight Fraction PVME (Bulk)	Weight Fraction PVME (Surface)	Surface Fraction PVME-f$_{PVME}$	Distribution Coefficient-K$_{PVME}$
0.05	0.567	0.573	11.3
0.20	0.769	0.773	3.8
0.50	0.933	0.935	1.9

parameter. Scaling theory[47] also predicts behavior represented by Eqn. (10), however in the attractive case the exponent, m, is equal to 1.25.

The experimental data (Figure 5) correspond qualitatively to the functional form given by Eqn. 10. An abrupt initial decrease in surface tension is observed, followed by a further decrease as the PVME concentration is increased. The concentration dependence is not linear as predicted by the mean field theories, however the data points are too few to establish whether they follow any particular power law dependence as given by (10). In addition, these theories were developed for polymer solutions, and are not completely applicable for polymer blends.

The concentration dependence of surface tension is also predicted by the parallel-layer model.[3,22,24] This approach assumes that the surface contains a monolayer of material in equilibrium with the bulk phase. Although physically unappealing, the theory has produced predictions which are in agreement with more sophisticated theories for polymer solutions.[46] In applying the theory, we assume that polystyrene is the solvent. In the case of polymer blends,[48] the ratio of molar volumes (i.e., r in reference 22) is taken as 15.5, and the lattice parameter a is set $(V_{PS}/N_O)^{2/3}$ where V_{PS} is the molar volume of polystyrene and N_O is Avogadro's number. Since the Flory-Huggins expression for free energy is employed in the theoretical development, only non-negative values of the interaction parameter, χ, are appropriate. The interaction parameters for PVME/PS blends in the miscible state are negative,[33,35,36] however the magnitude is small (ca. -1×10^{-4}), and we assume the mixture to be athermal (i.e., $\chi = 0$). The qualitative correspondence between the monolayer theory and experiment is excellent, as seen in Figure 5.

Proper account of the concentration dependence of surface tensions for our data would require an extension of the solutions theories that would be

appropriate for polymer blends. The framework for such a treatment has been presented by Poser and Sanchez[46] using the generalized square gradient approach. This treatment can account for the non-linear concentration dependence of surface tension for polymer solutions, but its application to miscible blends involves specification of two parameters associated with mixing rules for the polymer-polymer interaction energy and specific volume. In principle, values for these parameters may be determined experimentally, allowing direct calculation of the surface tension of the blend. The feasibility of this approach is current under consideration.

B. X-Ray Photoelectron Spectroscopy

Quantitative analysis of the XPS data focusses on resolution of the C_{1s} spectra for the PS/PVME blends. The C_{1s} spectra for pure PVME (Figure 6a) is a doublet containing contributions from carbon-oxygen (at 286.6 eV) and carbon-hydrogen bonds (at 285 eV). The C_{1s} spectra for PS (Figure 6b) shows only a singlet carbon-hydrogen peak and a small satellite peak at 291.6 eV due to a π to π^* shake-up transition.[49] Characteristics of the homopolymer core level spectra are given in Table III.

Typical data for the miscible blends (Figure 7) exhibit doublets as a result of superposition of the two homopolymer spectra. The surface composition can be extracted from these spectra by resolving the two contributions and calculating the integrated area under each peak.

The integrated intensity I_i of a core-electron photoemission spectrum is given by[50]

$$I_i = N_i S_i \tag{11}$$

Table III

Characteristics of XPS Core levels for PS and PVME

	C_{1s} (hydrogen)		C_{1s} (Oxygen)		C_{1s} ($\pi \to \pi^*$)	O_{1s}	
	BE	FWHM	BE	FWHM	BE	BE	FWHM
PS	285.0	1.40 ± 0.05			291.6 ± 0.1		
PVME	285.0	1.40 ± 0.05	286.6 ± 0.1	1.48 ± 0.05		533.2 ± 0.2	1.50 ± 0.05

BE = binding energy, FWHM = full width at half maximum.

where N_i is the average number of atoms per unit sampling volume and S_i is the sensitivity factor. The sensitivity factor for carbon atoms in two distinct chemical environments is approximately identical, and therefore the intensity ratio is equal to the average atomic ratio of the two types of carbon atoms. The area intensity ratio of oxygen to hydrogen carbon, calculated by a peak fitting program, can be expressed as

$$\frac{I_{CO}}{I_{CH}} = \frac{\dfrac{2\omega}{M_v}}{\dfrac{\omega}{M_v} + \dfrac{8(1-\omega)}{M_s}} \tag{12}$$

where ω is the average weight fraction of PVME within the sampling depth. M_s and M_v are the molecular weights of the styrene and vinyl methyl ether repeat units, respectively.

The photoemission peaks in the raw, uncorrected spectra, are superimposed over an inelastic scattering background. This background was estimated according to the method of Proctor and Sherwood.[51] After background subtraction, resolution of the C_{1s} spectra into the C-O and C-H contributions was accomplished by fitting a combination of Gaussian and Lorentzian intensity functions to the data. These distributions are defined by the peak maximum positions, full width at half maximum values, peak maximum intensities, and percentage of Gaussian. In practice, the peak regression for blend specimens was carried out by manually fixing the positions of the C-O and C-H peaks and the FWHM of the C-O peak; and subsequently calculating the FWHM of the C-H peak and the peak intensities by a non-linear regression algorithm. Initial values for these parameters were obtained by analysis of the pure PS and PVME homopolymers. The best fit was obtained by manual iteration on this procedure and was determined to be that set of parameters which gave the minimum sum of squared residuals normalized by the total sum of squares. The statistical error

inherent to the regression analysis leads to errors of $\pm$ 3-5 weight percent in the surface composition. This error is largest for grazing take off angles.

As the result of a relatively high source chamber pressure ~ 10^{-8} torr, a non-negligible hydrocarbon contamination layer is continuously deposited on the specimen during the experiment. The hydrocarbon contamination gives rise to a small contribution to the C_{1s} spectrum at 285.0 eV. Hydrocarbon contamination is a universal phenomena in XPS experiments that has been attributed to the heating of the x-ray source and the presence of diffusion pump oil at finite pressure.[52] While the atomic ratio of oxygen carbon to hydrogen carbon is exactly 2:1 for pure PVME, the measured ratio is found to be 2:(1+x) where x is positive and a function of time, t, and electron take off angle, θ. $x(\theta,t)$ was determined from measurements on pure PVME, and was assumed to be identical for all blend samples. With this assumption the contribution of the hydrocarbon contamination was accounted for in the analysis.

1.   Composition Dependence

The surface enrichment of PVME is dependent on the molecular weights of the blend constituents and the overall blend composition. This is illustrated in Fig. 8 where the "average" surface composition is given as a function of the overall blend composition. The "average" surface concentration reflects the total of all material residing in the sampling depth (~ 70Å). The relative amount of surface enrichment is represented by the distribution coefficients [see eqn. (9)] given in Table IV.

In general, the trends with changing composition are similar to those seen in the surface tension data. The magnitudes of the XPS distribution coefficients, however, are smaller than those from the surface tension analysis. This results primarily from the fact that XPS measurement samples the composition

Table IV

XPS Distribution Coefficients as a Function of Blend Composition and Polystyrene Molecular Weight

Weight Fraction PVME in Bulk	Distribution Coefficients		
	$M_{PS} = 127{,}000$	$M_{PS} = 3100$	$M_{PS} = 1200$
5	5	-	-
20	2.66	1.72	1.6
50	1.53	1.37	1.17
80	1.16	1.14	1.1

distribution integrated over a depth of ca. 70Å, while the surface tension data more appropriately reflect the composition of the outermost surface layer. In addition, the XPS measurements were carried out at room temperature, while the surface tension data were collected at elevated temperatures.

2. Molecular Weight Effects

At fixed composition, the surface enrichment of PVME becomes more dominant as the PS molecular weight increases. This behavior is a direct consequence of the molecular weight dependence of the PS surface energy. It is well known that homopolymer surface tension increases as the chain length is increased.[6] The driving force for PVME surface enrichment (i.e., $\gamma_{PS} - \gamma_{PVME}$) therefore becomes larger as the PS molecular weight is increased.

LeGrand and Gaines[53] have shown that the molecular weight dependence of homopolymer surface tension follows an empirical expression of the form

$$\gamma = \gamma_\infty - K_e/M_n^{2/3} \tag{13}$$

where M_n is the number average molecular weight. For polystyrene at 177°C, values of the empirical constant, K_e, and surface tension at infinite molecular weight have been reported as 372.7 dyn/cm (Dalton)$^{2/3}$ and 29.97 dyn/cm respectively.[54]

The relationship between the driving force for surface adsorption and the resultant surface composition is illustrated in Fig. 9. The blends contain PVME of fixed molecular weight (MW - 99,000, $M_w/M_n \simeq 2$) with PS of varying molecular weight. The compositions of these blends are all identical at 50% bwt. of PS. Surface compositions were calculated from XPS spectra obtained with a take-off normal to the surface and analyzed according to Eqn. (12). The theoretical driving

force, $\gamma_{PS} - \gamma_{PVME}$, was estimated by subtracting the measured surface tension for PVME (@ 177ºC) from the empirical expression (Eqn. 13) for PS surface tension.

Since $d\gamma/dT$ is essentially identical for the blends and homopolymers, the surface tension difference will be insensitive to the temperature. Thus, although the XPS spectra were obtained at room temperature, the calculated surface tension difference (@ 177ºC) should still be an appropriate value to use for comparison. The close correspondence between surface energy difference and surface composition suggests that the molecular weight dependence of surface composition should follow a functional form similar to that for surface tension (i.e. Eqn. 13). That is, for fixed PVME molecular weight, $\gamma_{PS} - \gamma_{PVME}$ is proportional to $M_n^{-2/3}$. It then follows that the average surface composition should exhibit the same molecular weight dependence. The empirical $M_n^{-2/3}$ molecular weight dependence is borne out by the XPS data on the 50% bwt PS blends as illustrated in Fig. 10. A least squares fit of this data yields an empirical expression for the surface weight fraction of PS of form

$$\omega_{PS} = 23.1 + 2.03 \times 10^3 / M_n^{2/3} \tag{14}$$

There was some concern during the measurements that the use of polydisperse poly(methyl vinyl ether) ($M_w/M_n \simeq 2$) could complicate the behavior as a result of surface fractionation of low molecular weight PVME molecules. The correspondence between surface energy difference and surface composition (Figure 9) suggests that fractionation of species according to molecular weight does not occur. Surface analyses of bimodal molecular weight blends of polystyrenes by secondary ion mass spectrometry[55] and by surface tension analysis[16] also failed to document any surface fractionation according to molecular weight.

3.   Surface Composition Profiles

The surface concentration gradient is amenable to characterization by XPS experiments. Concentration depth profiling can be accomplished by changing the photoelectron take-off angle to the analyzer[56,57] as depicted schematically in Figure 11. The sampling depth of XPS is limited by the effective mean free path for electrons escaping from the surface. At take-off normal to the surface, the effective sampling depth is a maximum, given approximately by $z \simeq 3\lambda$ where λ is the mean free path. When non-normal take-off angles are used, the sampling depth decreases according to

$$Z \simeq 3 \lambda \cos \theta \qquad (15)$$

where θ is the angle between the sample normal and the emitted electron path to the analyzer as shown in Figure 11. Approximately 95% of the photoelectrons detected in the experiment emanate from the sampling depth defined in this fashion.

Accurate knowledge of the electron mean free path is vital to the quantitative success of XPS depth profiling, however there is considerable discrepancy in the literature values for λ. Electron mean free paths for polymers have been discussed in detail by Clark.[58] Following their conclusions, we have chosen to use the value $\lambda = 23 \pm 3 \text{Å}$. This value was also obtained by Szajman et. al[59].

Hydrocarbon contamination and surface roughness[60] also lead to uncertainty in the value of z, especially at grazing angles. The effects of hydrocarbon contamination are minimized by using fresh samples for every pair of take-off angles, and by subtracting a hydrocarbon signal $x(\theta,t)$ estimated from experiments on pure PVME as discussed earlier in this paper. Even with these

precautions, the errors in the experimental integrated surface compositions for small z are considerable. Application of the substrate overlayer model to this data furnishes a maximum thickness of 3Å for the contamination layer.

Representative angle dependent C_{1s} core-level spectra for a 50/50 PS/PVME blend are shown in Fig. 12. Analysis of this data according to Eqn. (12) gives the corrected average surface composition as a function of effective sampling depth as shown in Fig. 13. This profile is in good agreement with data on a similar specimen reported by Pan and Prest.[31] The PVME surface concentration increases smoothly from the bulk value to attain a value of ca 98% in the outermost surface layer. Similar behavior is observed for 5/95 and 20/80 blends (Figs. 14 & 15).

The XPS depth profile data does not furnish a direct measurement of the surface composition gradient. Due to the nature of the XPS experiment, the surface composition measured is actually an integral value of the composition averaged over the sampling depth. For the core-level spectra of a particular atomic species, the photoelectron intensity for core-level j at take-off angle θ may be expressed as[56]

$$I_j(\theta) \sim \int_0^\infty n_j(z) \exp(-z/\lambda_j \cos\theta)\, dz \tag{16}$$

where $n_j(z)$ represents the atomic composition depth profile for the species of interest (e.g., C-O or C-H in the present case).

For the PVME/PS blends, we have calculated the average surface weight fractions as a function of sampling depth through application of equation (12) to angle-dependent XPS spectra. To accomplish this, a model for the concentration gradient, $n_j(z)$, is required; whereupon the intensities $I_j(\theta)$ can be determined by (16) and the average surface composition profile $\omega(z)$ can be calculated through

Eqn. (12). This profile can be compared directly to an experimental profile such as is given in Figures 13-15.

Some of the theories that were discussed previously for surface tension of polymer solutions also make predictions for the concentration gradient at the air-solution interface. For an attractive interface, the predicted concentration profile is[25]

$$\phi(z) = \phi_b \coth^2[(z/\xi) + \alpha] \tag{17}$$

where ξ is the Edwards correlation length[61,62] and α is a constant related to the surface density.

The experimental integrated profiles are modelled by using this profile in expression (16). The results are shown in Figures 13-15. For all cases studied, the concentration profile predicted by the mean field solution theories compares well with the experimental data for the miscible blends. The resultant fit parameters are summarized in Table V.

The concentration dependence of the screening length, ξ, in polymer solutions is predicted by several theories[61-64] and is a function of the concentration regime of the phase diagram. Unfortunately, the data in Table V do not cover a large concentration regime, and are not of sufficient accuracy or precision to examine the correspondence with the theoretical predictions.

The magnitude of the screening legnths are reasonable however. The theoretical screening legnth is bounded by the PVME radius of gyration (for low concentrations) and the statistical segment length of PVME (for bulk PVME).

Table V

Composition Gradient Parameters
For Blends of PVME ($M_w = 99,000$) and PS

Wt. Fraction PVME	ξ(nm)	α	$\phi(z=0)$
0.05	5.0	0.28	0.65
0.20	3.5	0.51	0.90
0.50	7.0	0.89	0.98

Values of these limits for similar blends have been reported as 9.7nm[65] and 0.35nm [66], respectively. The experimental screening lengths do fall within these limits.

Extensions of the Sanchez-Poser[46] treatment could again be applied to model the concentration profiles, however we do not have sufficient experimental data to properly accomplish this at the present time.

SUMMARY

The surface character of miscible PVME/PS blends has been examined as a function of the overall blend compositions, the constituent molecular weights, and the temperature. Surface tension data and XPS analysis demonstrates substantial surface enrichment of PVME for all of the blends examined and under all tested conditions. The PVME exhibits strong surfactant behavior, causing a dramatic reduction in surface tension when even small quantities are added. By comparison of XPS and surface tension data, we show a direct correspondence between the driving force for surface segregation (i.e., the surface energy difference between PS and PVME) and the resultant surface composition. This relationship is emphasized by the results of XPS measurements of the molecular weight dependence of the surface composition. An empirical $M_n^{-2/3}$ power law dependence of surface composition is observed, reflecting clearly the empirical $M_n^{-2/3}$ dependence of the surface energy difference. Surface composition gradients determined by angle-dependent XPS experiments are well represented by the profiles predicted by mean field theories of polymer solutions. The experimental profiles indicate that the PVME content of the outermost surface layer increases with the bulk PVME content, and attains values as high as 98 percent for certain blends. The combination of x-ray photoelectron spectroscopy for determination of surface structure and pendant drop measurements of surface

tension for characterization of surface thermodynamics constitutes an extremely powerful means for the investigation of the surface properties of polymeric materials.

ACKNOWLEDGEMENT

REFERENCES

1. Blakely, J.M. in Chemistry and Physics of Solid Surfaces, Vol. 2, ed. R. Vanselow, CRC Press, Inc., 1979.

2. Carey, B.S.; Scriven, L.E.; Davis, H.T. AICHE Journal 1980, 26, 705.

3. Defay, R.; Prigogine, I.; Bellemans, A. Surface Tension and Adsorption; John Wiley and Sons, New York, 1951.

4. Thomas, H.R.; O'Malley, J.J. Macromolecules 1981, 14, 1316.

5. Schmitt, R.L.; Gardella, Jr., J.A.; Salvati, L. Macromolecules 1986, 19, 648.

6. Wu, S. Polymer Interface and Adhesion; Dekker, New York, 1982.

7. Rastogi, A.K.; St. Pierre, L.E. J. Colloid Interface Sci. 1969, 31, 168.

8. Owen, M.J.; Kendrick, J.C. Macromolecules 1970, 3, 458.

9. Clark, D.T.; Peeling, J.; O'Malley, J.J. J. Polym. Sci: Polym. Chem. Ed. 1976, 14, 543.

10. Thomas, H.R.; O'Malley, J.J. Macromolecules 1979, 12, 323.

11. O'Malley, J.J.; Thomas, H.R.; Lee, G.M. Macromolecules 1979, 12, 966.

12. Schmitt, R.L.; Gardella, Jr., J.A.; Magill, J.H.; Salvati, Jr., L.; Chin, R.L. Macromolecules 1985, 18, 2675.

13. McGrath, J.E.; Dwight, D.W.; Riffle, J.S.; Davidson, T.F.; Webster, D.C.; Vishwanathan, R.; Polym. Prepr. Am. Chem. Soc., Div. Polym. Chem. 1979, 20(2), 528.

14. Gervais, M.; Douy, R.; Gallot, B.; Erre, R. Polymer 1986, 27, 1513.

15. Kugo, K.; Hata, Y.; Hayashi, T.; Nakajima, A. Polym. J. 1982, 14, 401.

16. Gaines, Jr., G.L.; Bender, G.W. Macromolecules 1972, 5, 82.

17. Yamashita, Y. J. Macromol. Sci.-Chem. 1979, A13(3), 401.

18. Owens, D.K. J. Appl. Polym. Sci. 1970, 14, 185.

19. Kendrick, T.C.; Kingston, B.M.; Lloyd, N.C.; Owen, M.J. J. Colloid Interface Sci. 1967, 24, 135.

20. Gaines, Jr., G.L. Macromolecules 1981, 14, 1366.

21. Fredrickson, G., to be published.

22. Gaines, Jr., G.L. J. Phys. Chem. 1969, 73, 3143.

23. Gaines, Jr., G.L. J. Polym. Sci., 1969, A2, 7.

24. Siow, K.S.; Patterson, D. J. Phys. Chem. 1973, 74, 356.

25. Ober, R.; Paz, L.; Taupin, C.; Pincus, P.; Boileau, S. Macromolecules 1983, 16, 50.

26. DiMeglio, J.M.; Ober, R.; Paz, L.; Taupin, C.; Pincus, P.; Boileau, S. J. Physique 1983, 44, 1035.

27. Koberstein, J.T. in Encyclopedia of Polymer Science and Engineering, John Wiley, Vol. 8, 1987, pg. 237.

28. Busscher, et. al., Polym. Commun. 1985, 26, 252.

29. LeGrand, D.G.; Gaines, Jr., G.L. J. Polym. Sci., 1971, C34, 45.

30. Flory, P.J. Principles of Polymer Chemistry, Cornell University Press, 1953.

31. Pan, D. H-K.; Prest, Jr., W.M. J. Appl. Phys. 1985, 58(8), 15.

32. McMaster, L.P. Macromolecules 1973, 6, 760.

33. Nishi, T.; Wang, T.T.; Kwei, T.K. Macromolecules 1975, 8, 227.

34. Kwei, T.K.; Wang, T.T.; in Polymer Blends, Paul, D.R.; Newman, S. Eds., Academic, New York, 1978, Vol. 1.

35. Hadziioannou, G.; Stein, R. Macromolecules 1984, 17, 567.

36. Shiomi, T.; Kohno, K.; Yoneda, K.; Tomita, T.; Miya, M.; Imai, K. Macromolecules 1985, 18, 414.

37. Jelenic, T.; Kirste, R.G.; Oberthuer, R.C.; Schmitt-Streeker, S.; Schmitt, B.J. makromol. Chem. 1984, 12, 185.

38. Bhatia, Q.S.; Chen, J.K.; Koberstein, J.T.; Sohn, J.T.; Emerson, J.E. J. Colloid Interface Sci. 1985, 106, 352.

39. Anastasiadis, S.H.; Chen, J.K.; Koberstein, J.T.; Sohn, J.T.; Emerson, J.E. Polym. Eng. Sci. 1986, 26, 1410.

40. Anastasiadis, S.H.; Chen, J.K.; Koberstein, J.T.; Sohn, J.T.; Emerson, J.E.; Siegel, A.F. J. Colloid Interface Sci., in press.

41. Bender, Gl.W.; Gaines, Jr., G.L. Macromolecules 1970, 3, 128.

42. Van Krevelen, D.W. Properties of Polymers, Elsevier, Amsterdam, 1976.

43. Kwei, T.K.; Nishi, T.; Roberts, R.F. macromolecules 1974, 7, 667.

44. Hartland, S.; Hartley, R.W. Axisymmetric Fluid-liquid Interface, Elsevier, Amsterdam, 1976.

45. Cahn, J.W. J. Chem. Phys. 1977, 66, 3667.

46. Poser, C.I.; Sanchez, I.C. Macromolecules 1981, 14, 361.

47. DeGennes, P.G. Macromolecules 1981, 14, 1637.

48. Bhatia, Q.S. Surface Studies of Homopolymers and Miscible Polymer Blends, Ph.D Thesis, Princeton University, 1987.

49. Clark, D.T.; Dilks, A. J. Polym. Sci., Polym. Chem. Ed. 1976, 14, 533.

50. Wagner, C.D.; Riggs, W.M.; Davis, L.E.; Moulder, J.F.; Muilenberg, J.E. Handbook of X-ray Photoelectron Spectroscopy, Perkin-Elmer Corp., 1979.

51. Proctor, A.; Sherwood, P.M.A. Anal. Chem. 1982, 54, 13.

52. Clark, D.T.; Thomas, H.R.; Dilks, A.; Shuttleworth, D.J. Electron Spectrosc. Relat. Phenomena, 1971, 10, 435.

53. LeGrand, D.G.; Gaines, Jr., G.L. J. Colloid Interface Sci. 1969, 31, 162.

54. Wu, S., in Polymer Blends; Paul, D.R.; Newman, S. eds., Academic, New York, 1978.

55. Goldblatt, R.D.; Scilla, G.J.; Park, J.M.; Johnson, J.N.; Huang, S. J. Appl. Polym. Sci., in press.

56. Fadley, C.S.; Bergström, S.A.L. Phys. Lett. 1971, 35A, 375.

57. Fadley, C.S. Prog. in Surf. Sci. 1984, 16, 275.

58. Clark, D.T.; Thomas, H.R. J. Polym. Sci. Polym. Chem. Ed. 1977, 15, 2843.

59. Szajman, J.; Liesegang, J.; Jenkin, J.G.; Leckey, R.G.G. J. Electron Spectrosc. Relat. Phenomena 1978, 14, 247.

60. Fadley, C.S.; Baird, R.J., Sickhaus, W.; Novakov, T.; Bergström, S.A.L. J. Electron Spectrosc. 1974, 4, 93.

61. Edwards, S.F. Proc. Phys. Soc., London, 1966, 88, 265.

62. Edwards, S.F. and Jeffers, E.F., J. Chem. Soc. (Faraday Transaction II) 1979, 75, 1020.

63. Daoud, M.; Jannink, G. Phys. (Paris) 1975, 37, 973.

64. Schaefer, D.W. Polymer 1984, 25, 387.

65. Hashimoto et. al., unpublished results quoted by Schichtel and Binder, Macromolecules, 20, 1679 (1987).

66. D. Schwan et al., J. Chem. Phys. in press.

FIGURE CAPTIONS

Figure 1.   Block diagram of the automated pendant drop apparatus.

Figure 2.   Pendant drop profile analysis of 95/05 w/w PS/PVME blend. (a) Digitized image; (b) Drop profile obtained by global thresholding; (c) Theoretical profile from robust shape comparison (line); experimental profile (diamonds).

Figure 3.   Pendant drop geometry.

Figure 4.   Surface tension of miscible blends of PS (3100), PVME homopolymers and blends. PVME homopolymer (open circles) PS/PVME 50/50 w/w (filled circles); 80/20 w/w (filled squares) PS/PVME; 95/05 w/w (filled triangles) PS/PVME; PS (3100) homopolymer (open squares).

Figure 5.   Surface tension of PS (3100)/PVME at 150°C as a function of bulk weight % PVME. Solid line is the monolayer theory [22] prediction with $\chi = 0$ and $a/kT = 0.49$ $(dyn/cm)^{-1}$. Dashed line is the expected result in the absence of preferential surface adsorption.

Figure 6. C_{1s} and O_{1s} spectra for polystyrene and poly(vinyl methyl ether) homopolymers.

Figure 7. C_{1s} and O_{1s} core level spectra for the miscible PS/PVME blends. (a) 95/05; (b) 80/20; (c) 50/50; (d) 20/80. Dashed lines indicate the individual peak contributions obtained from curve resolution. The brackets denote a signal of 100 cts./sec.

Figure 8.   Average surface weight % versus bulk weight % PVME. PS constituent of molecular weight = 127k (circles); PS molecular weight = 3100 (triangles); PS molecular weight = 1200 (squares).

Figure 9.   (a) Surface tension difference between PS and PVME hompolymers versus molecular weight of PS; (b) Average surface weight % PVME obtained from XPS versus molecular weight of PS.

Figure 10.   Average surface weight % PVME obtained from XPS versus (molecular weight of PS)$^{-2/3}$.

Figure 11.   Schematic diagram of angle-dependent XPS experiment for depth
             profiling studies. z = effective sampling depth, and λ = electron
             mean free path.

Figure 12. C_{1s} XPS spectra as a function of take off angle, θ for the miscible
             50/50 w/w PS/PVME blend. (a) 0°; (b) 30°; (c) 50°; (d) 60°; (e) 70°; (f)
             80°. Dashed lines are the results of curve resolution.

Figure 13.   Integral surface composition profile of 50/50 w/w miscible PS/PVME
             blend determined by angle-dependent XPS (circles). Solid line is the
             fit obtained by using $\coth^2 (z/\xi+\alpha)$ profile in expression (16), where ξ
             = 7.0 nm and α = 0.89. Dashed line is the $\coth^2 (z/\xi+\alpha)$ profile.

Figure 14.   Integral surface composition profile of 80/20 w/w miscible PS/PVME
             blend determined by angle-dependent XPS (circles). Solid line is the
             fit obtained by using $\coth^2 (z/\xi+\alpha)$ profile in expression (16), where ξ
             = 3.5 nm and α = 0.51. Dashed line is the $\coth^2 (z/\xi+\alpha)$ profile.

Figure 15.   Integral surface composition profile of 80/20 w/w miscible PS/PVME
             blend determined by angle-dependent XPS (circles). Solid line is the
             fit obtained by using $\coth^2 (z/\xi+\alpha)$ profile in expression (16), where ξ
             = 5.0 nm and α = 0.28. Dashed line is the $\coth^2 (z/\xi+\alpha)$ profile.

```
        ┌─────────────────┐
        │   Illumination  │
        │     Source      │
        └─────────────────┘
                 │
                 ▼
        ┌─────────────────┐
        │  Environmental  │
        │     Chamber     │
        └─────────────────┘
                 │
                 ▼
        ┌─────────────────┐
        │      Video      │
        │     Camera      │
        └─────────────────┘
                 │
                 ▼
┌──────────┐  ┌──────────────┐  ┌──────────────┐
│  Video   │◄─│ Frame Grabber│─►│ Mini-computer│
│ Monitor  │  │              │  │              │
└──────────┘  └──────────────┘  └──────────────┘
```

Fig 1

a

b

c

Fig :

Fig 3

Fig 4

Fig. 5

Fig. 6

C$_{1S}$ O$_{1S}$

INTENSITY(arb. units)

a

b

c

d

295   290   285   535   530
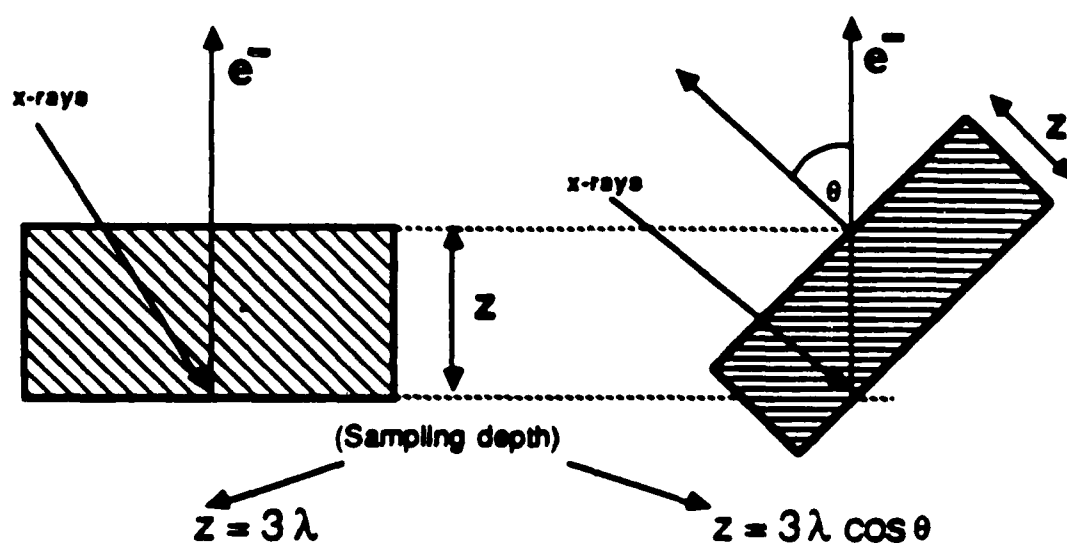BE (eV)   BE (eV)
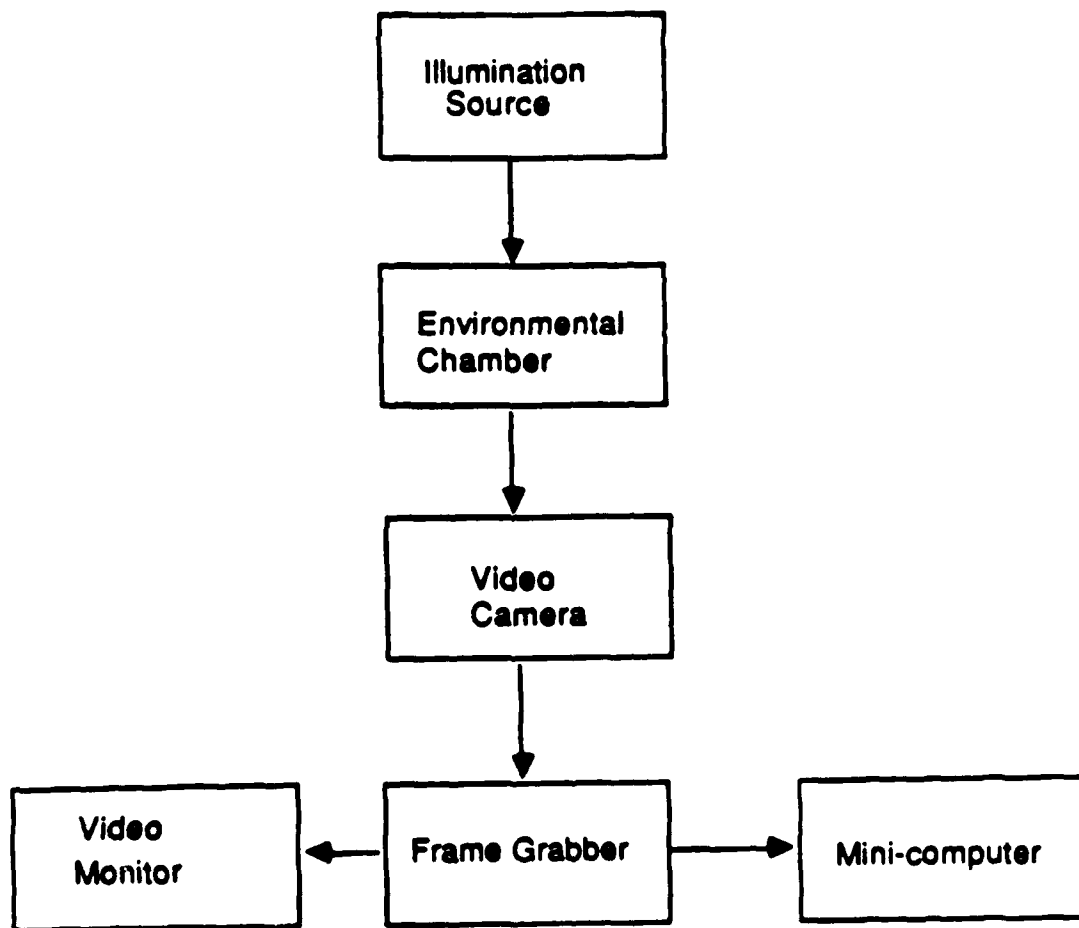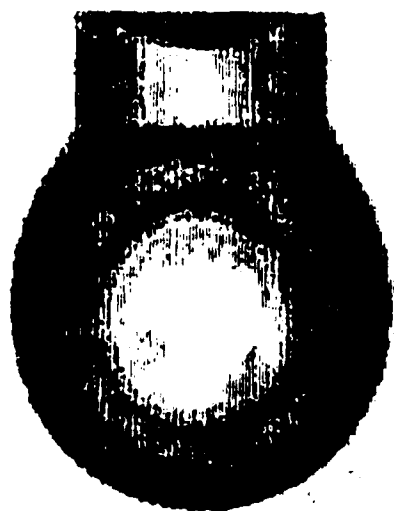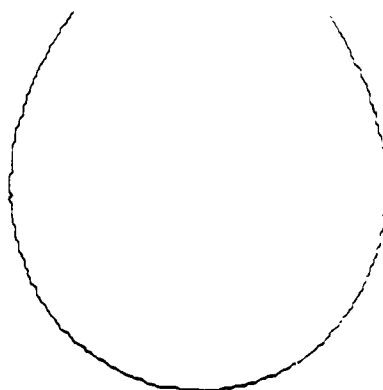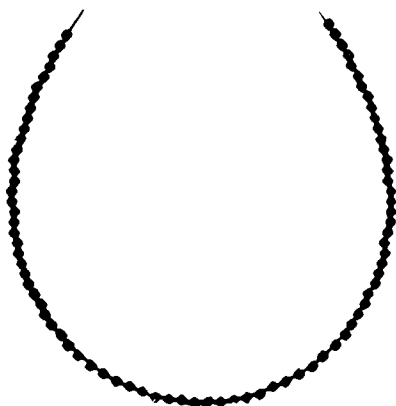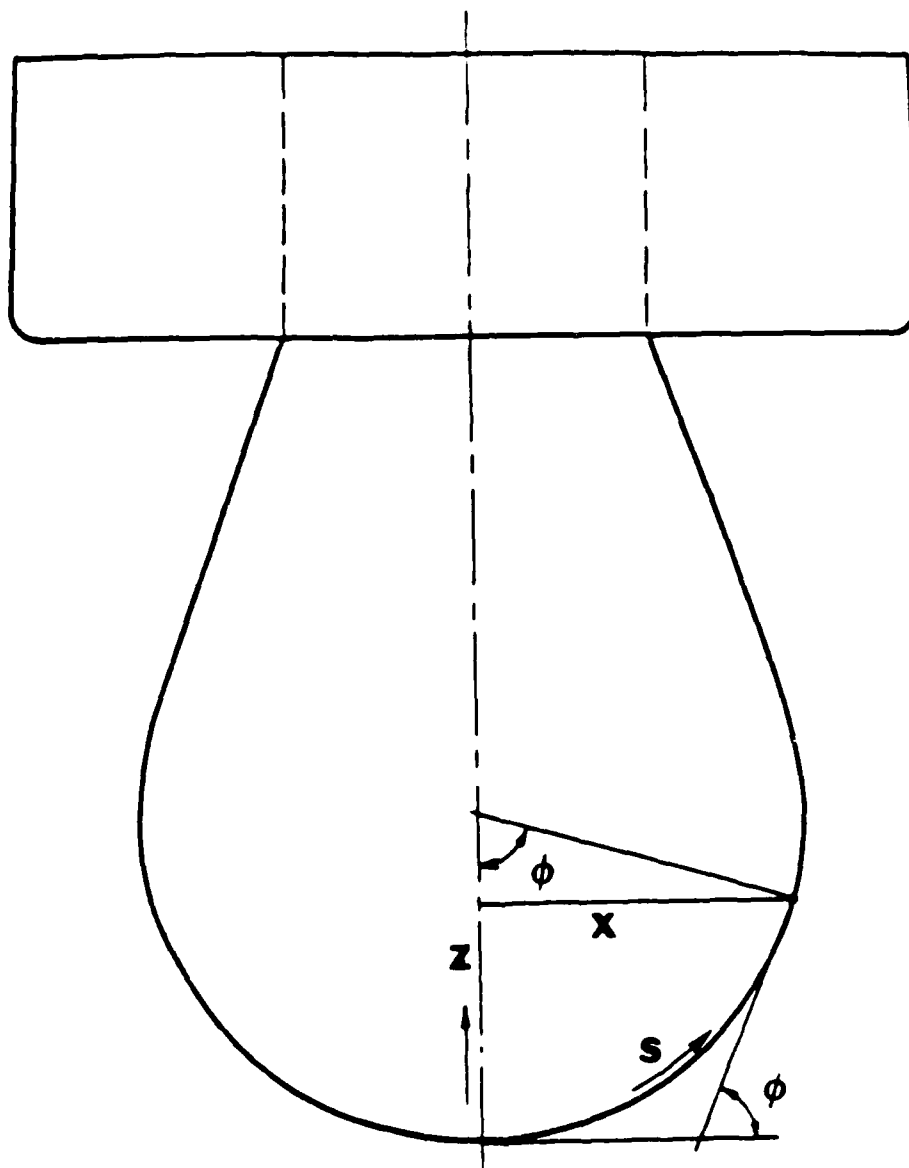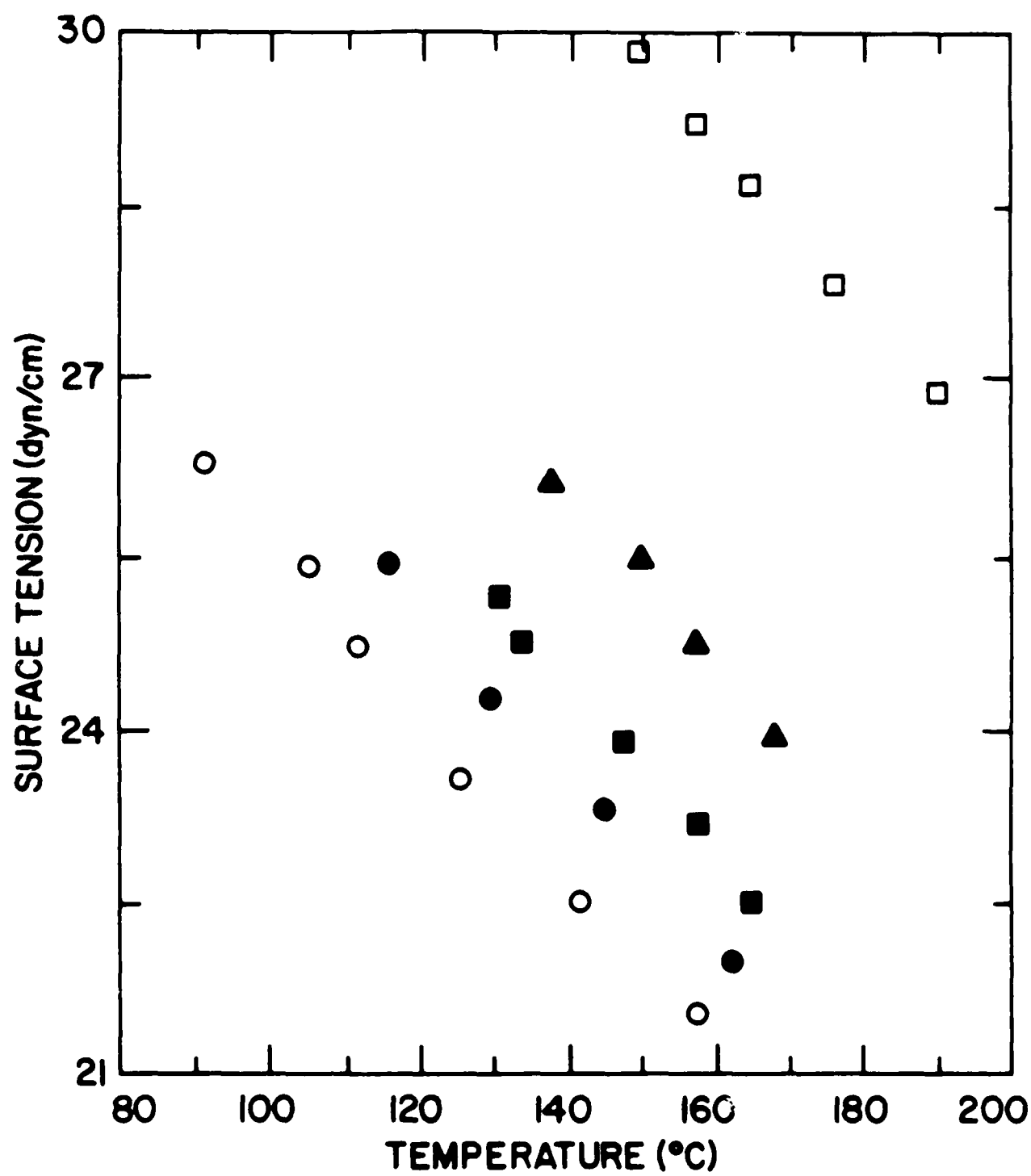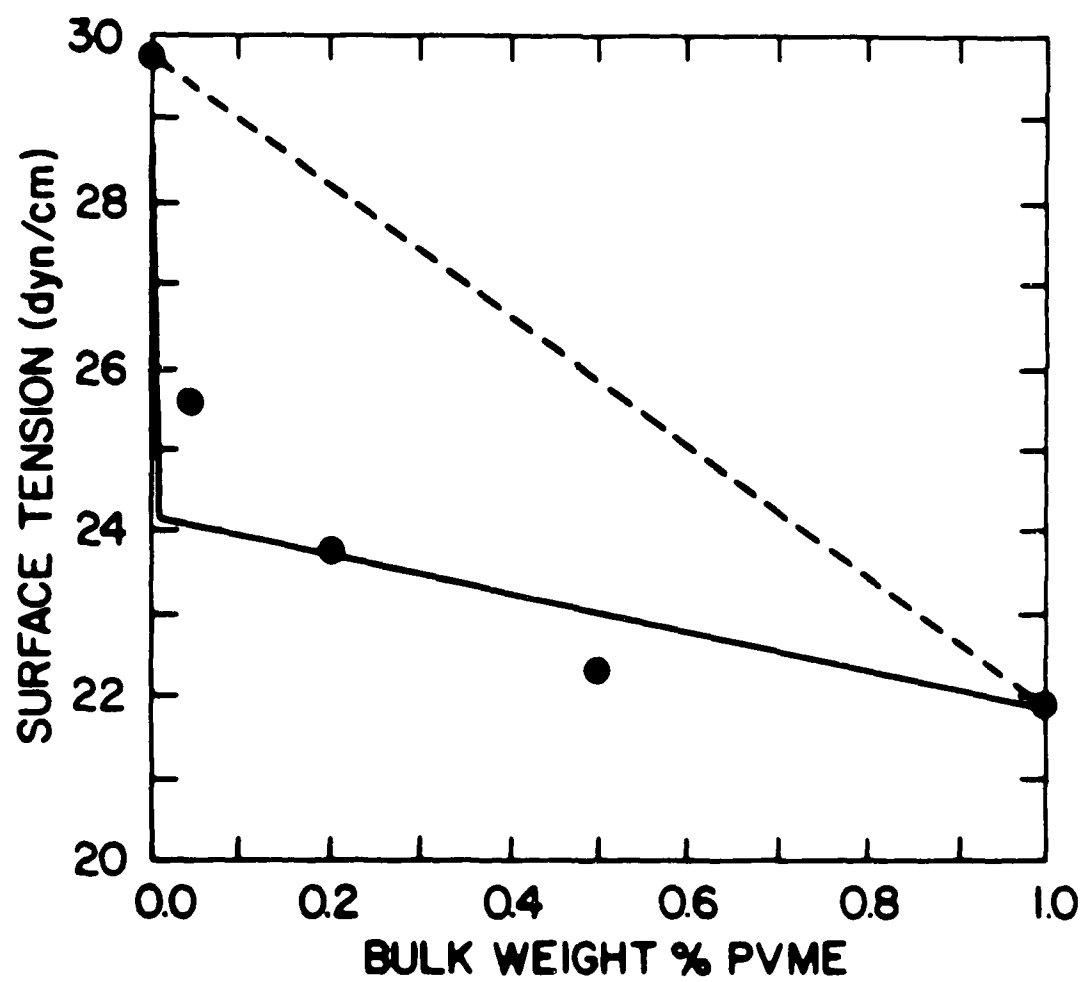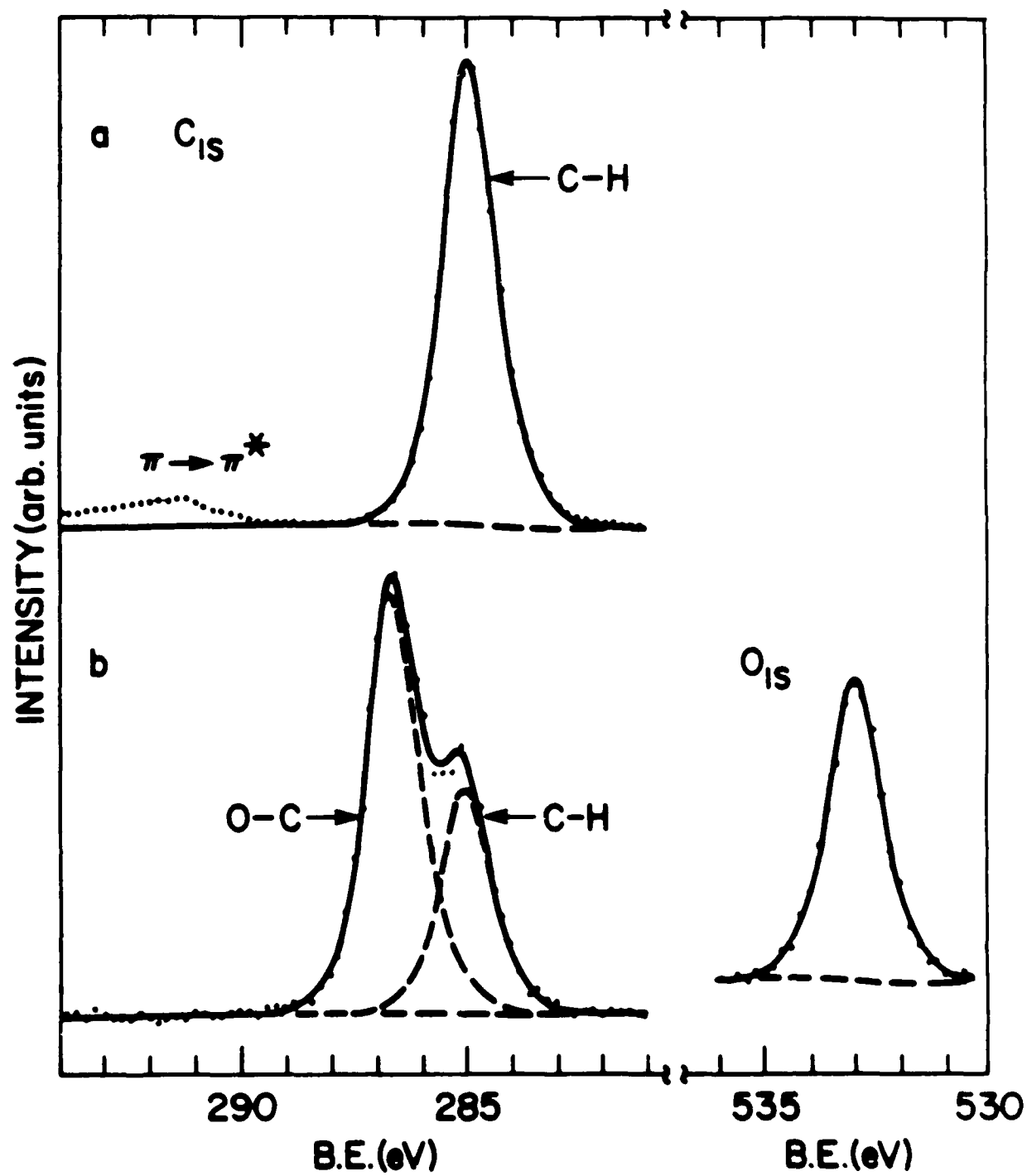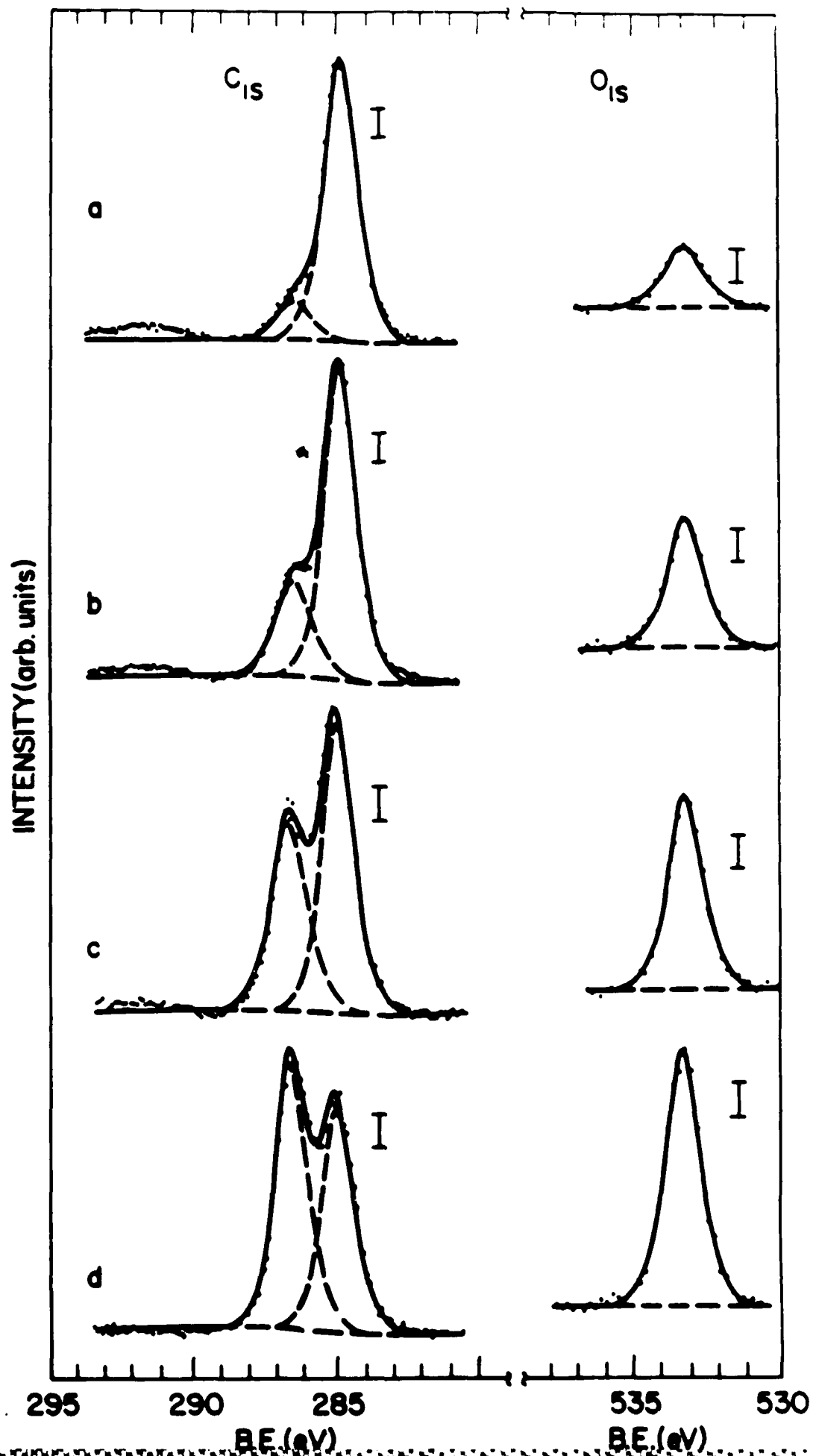
Fig. 7

Fig. 8

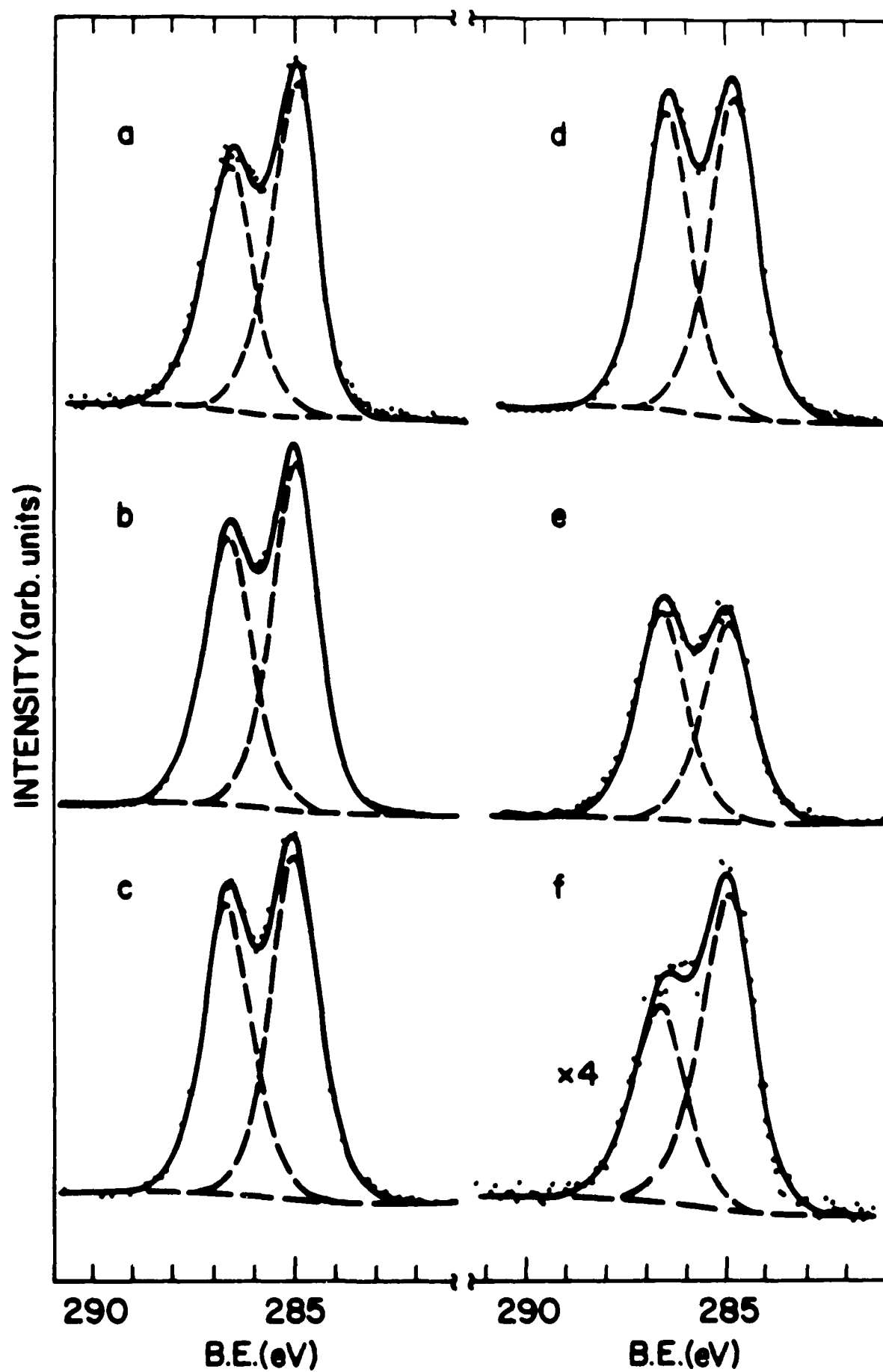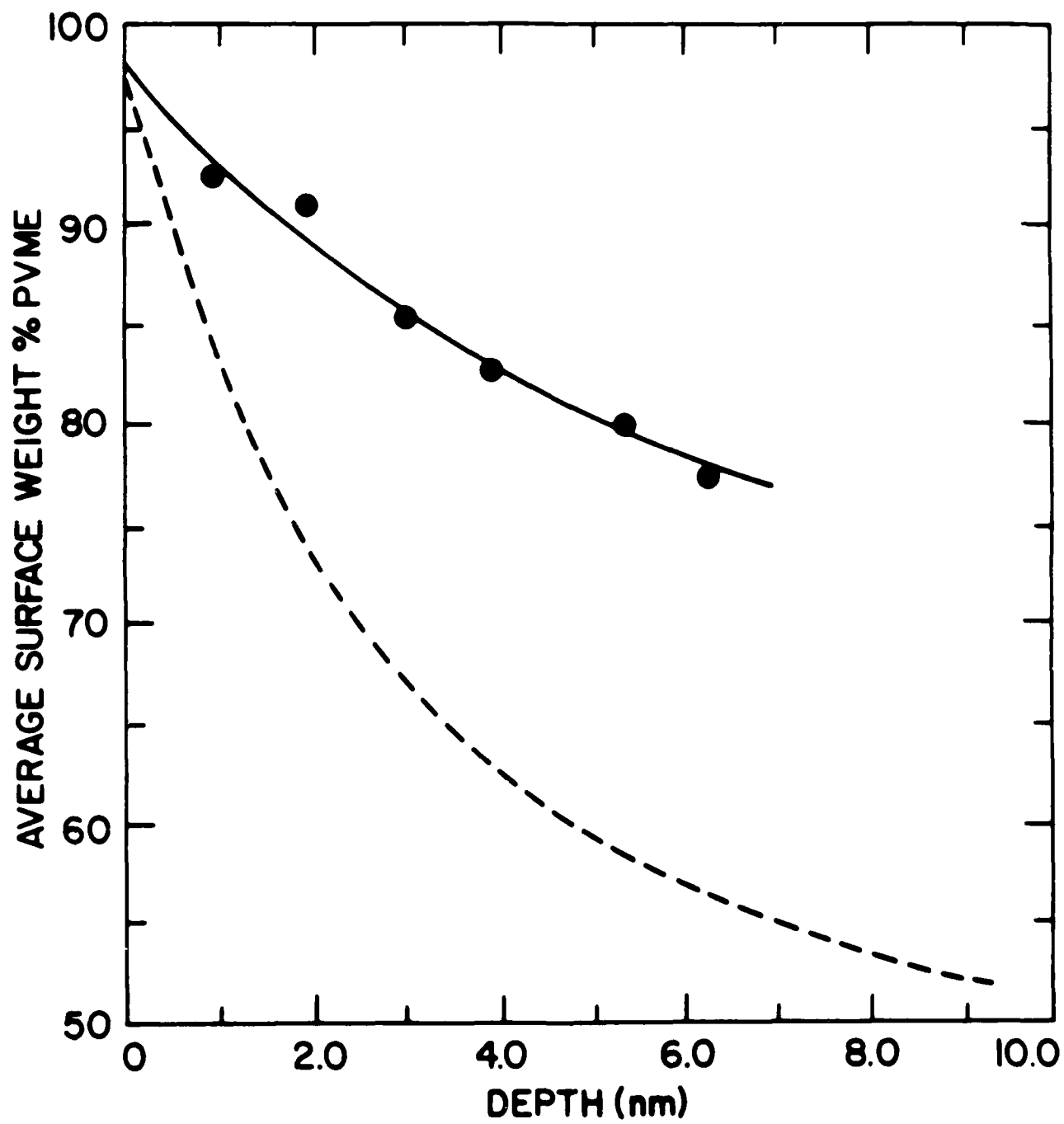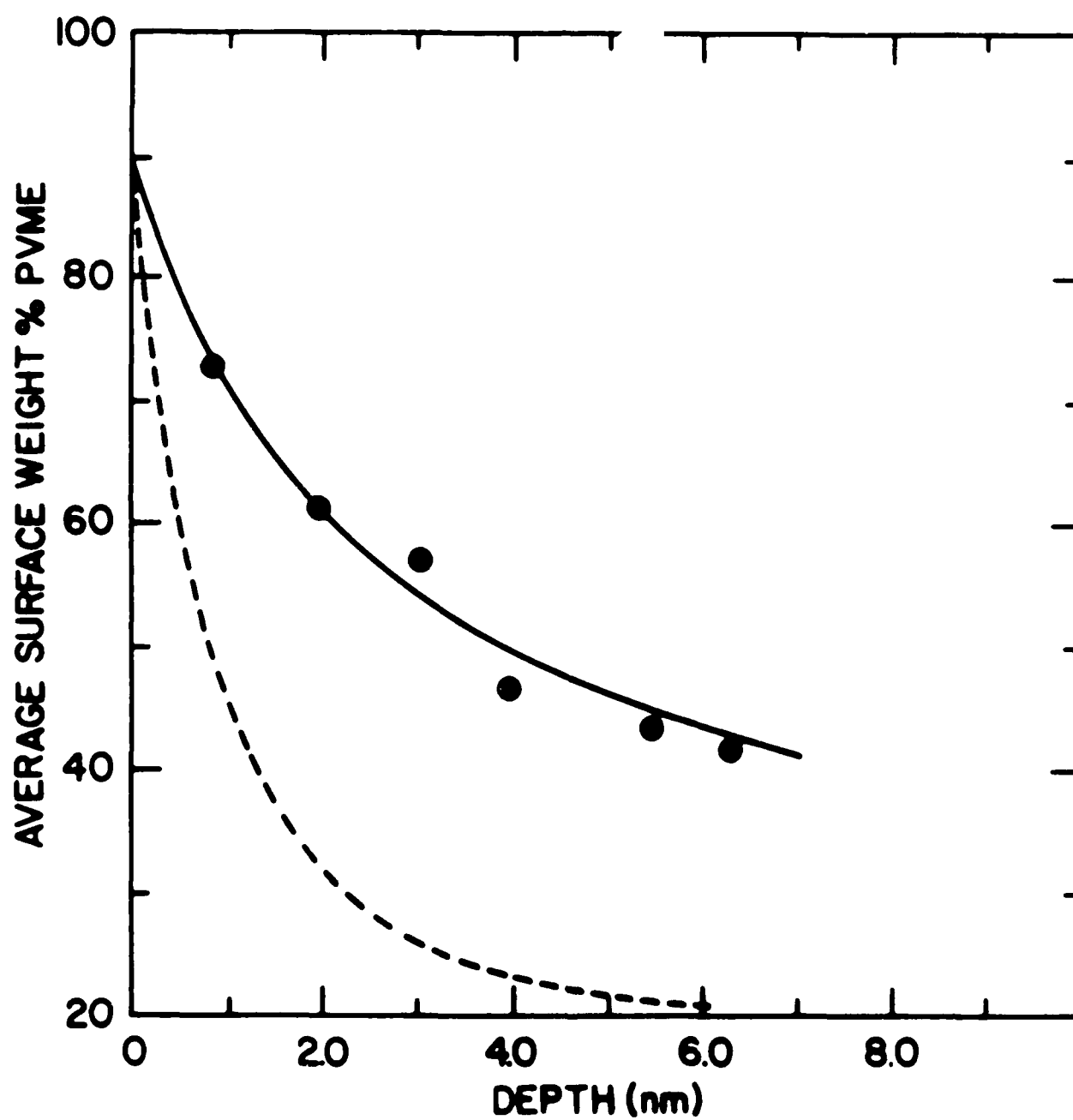Fig. 9

Fig. 10

Fig. 11
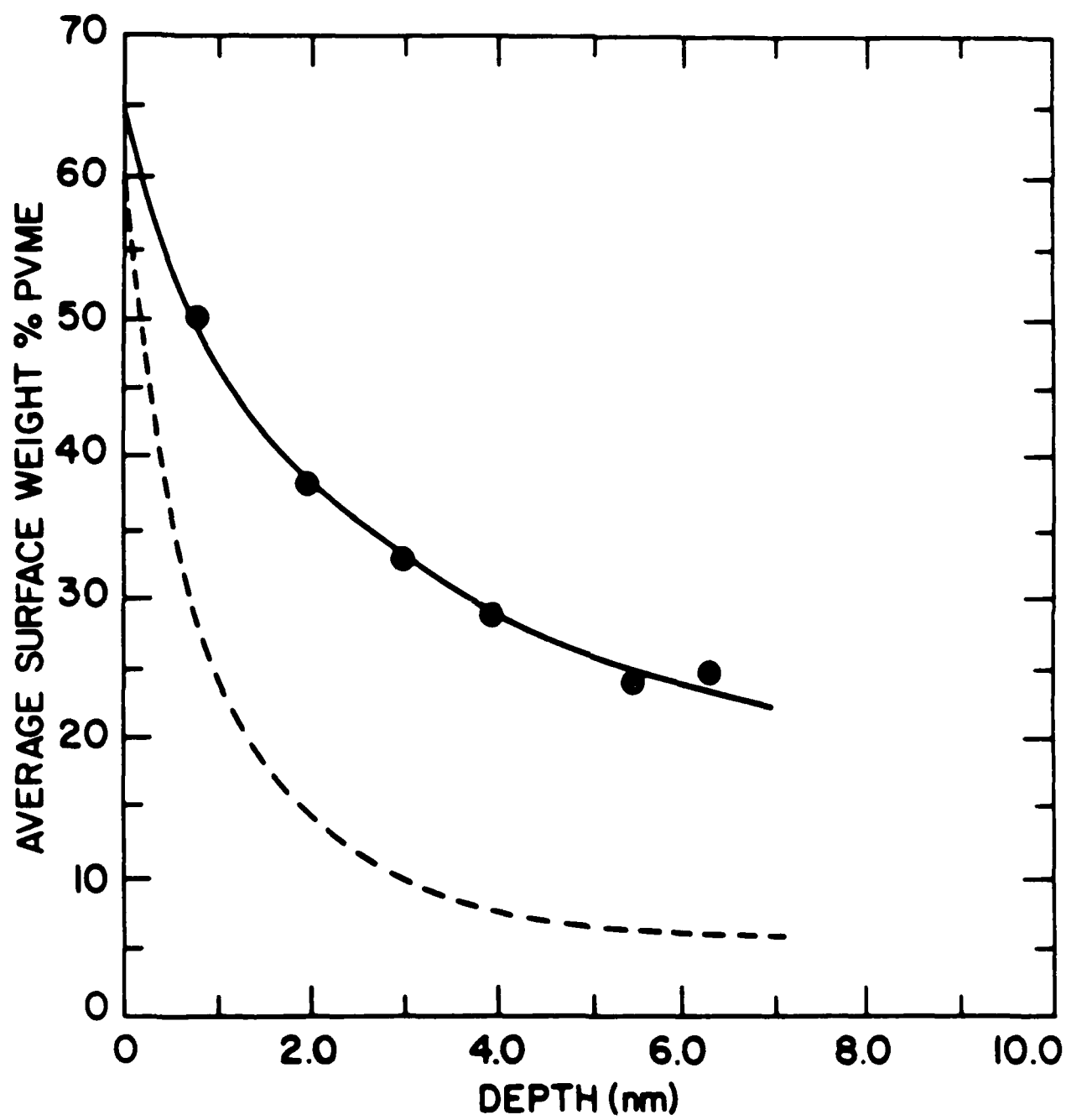
INTENSITY(arb. units)

B.E.(eV)   B.E.(eV)
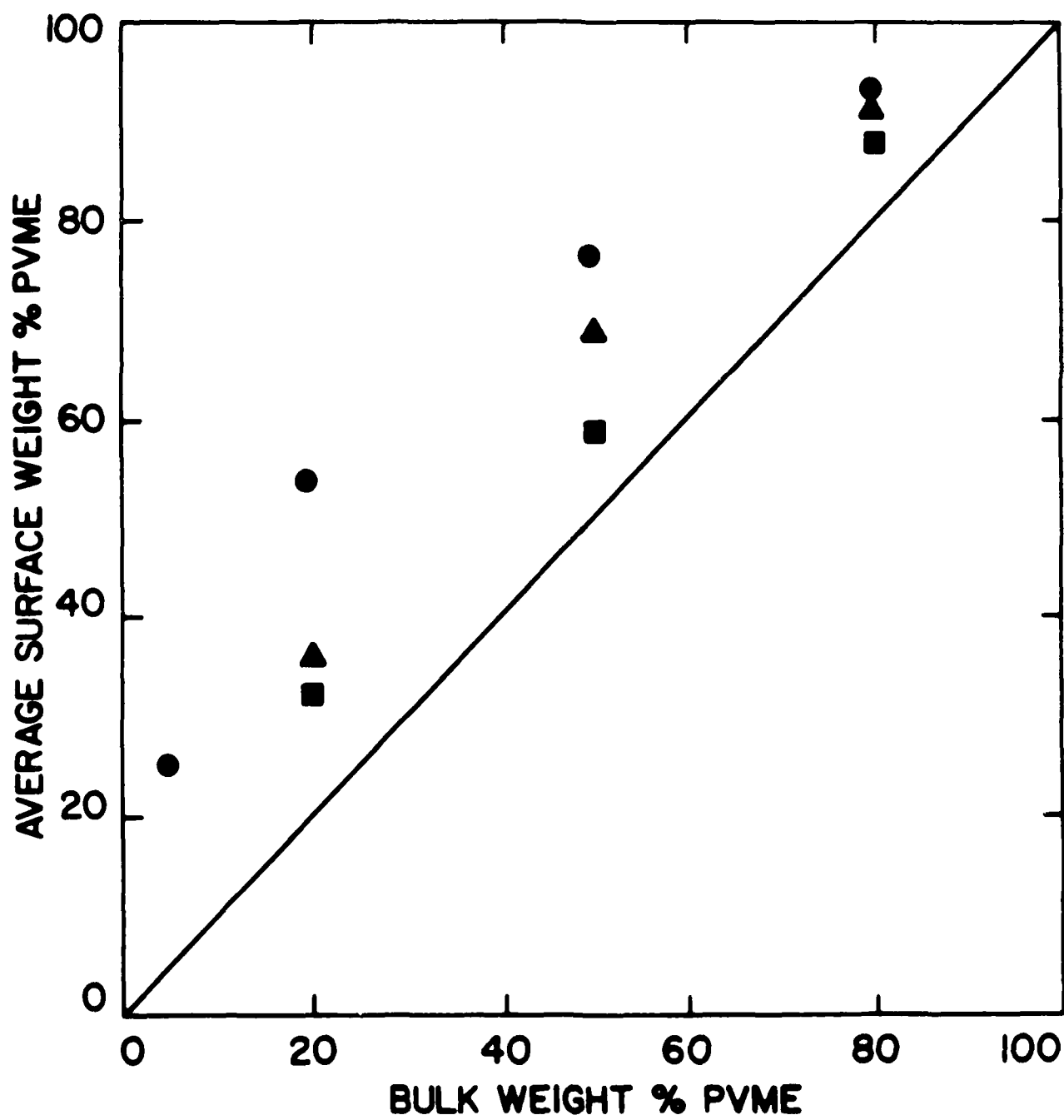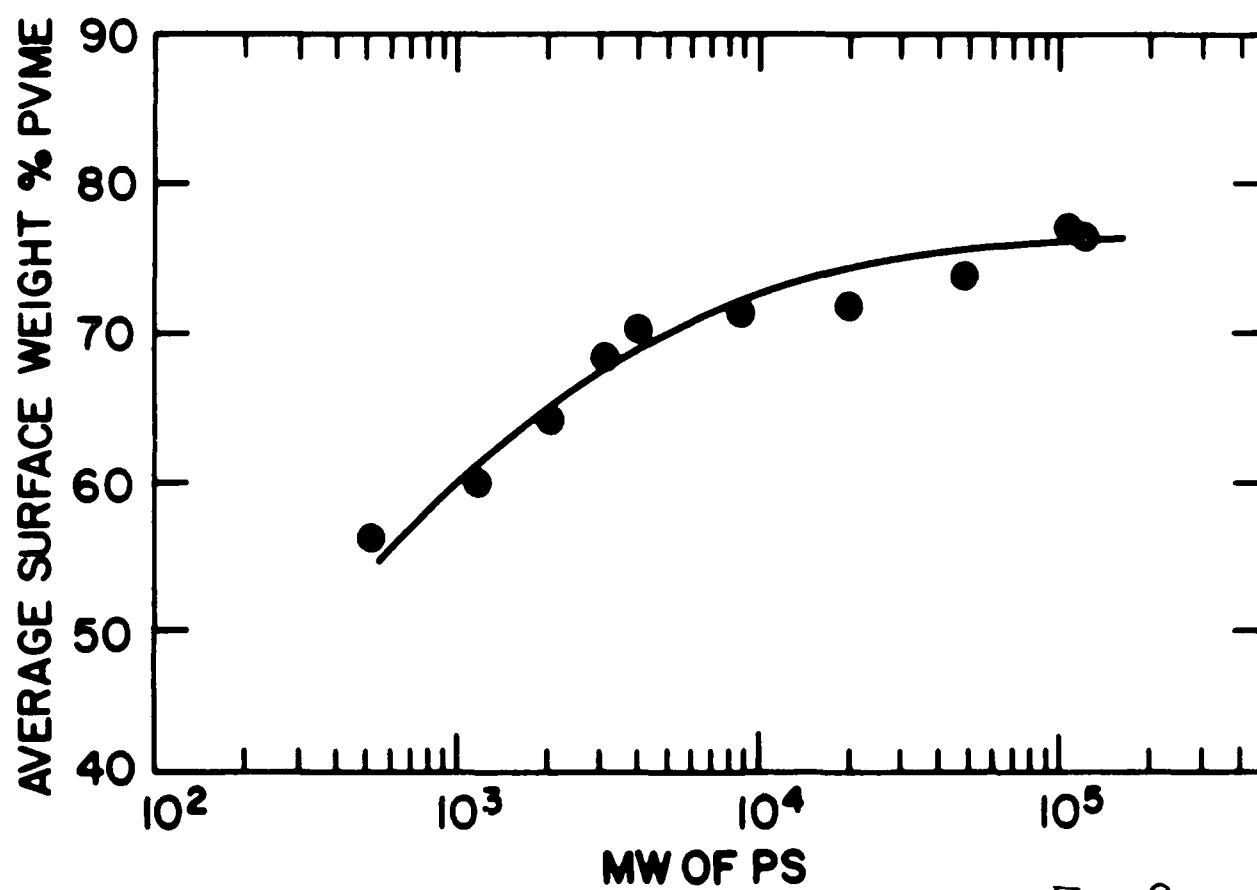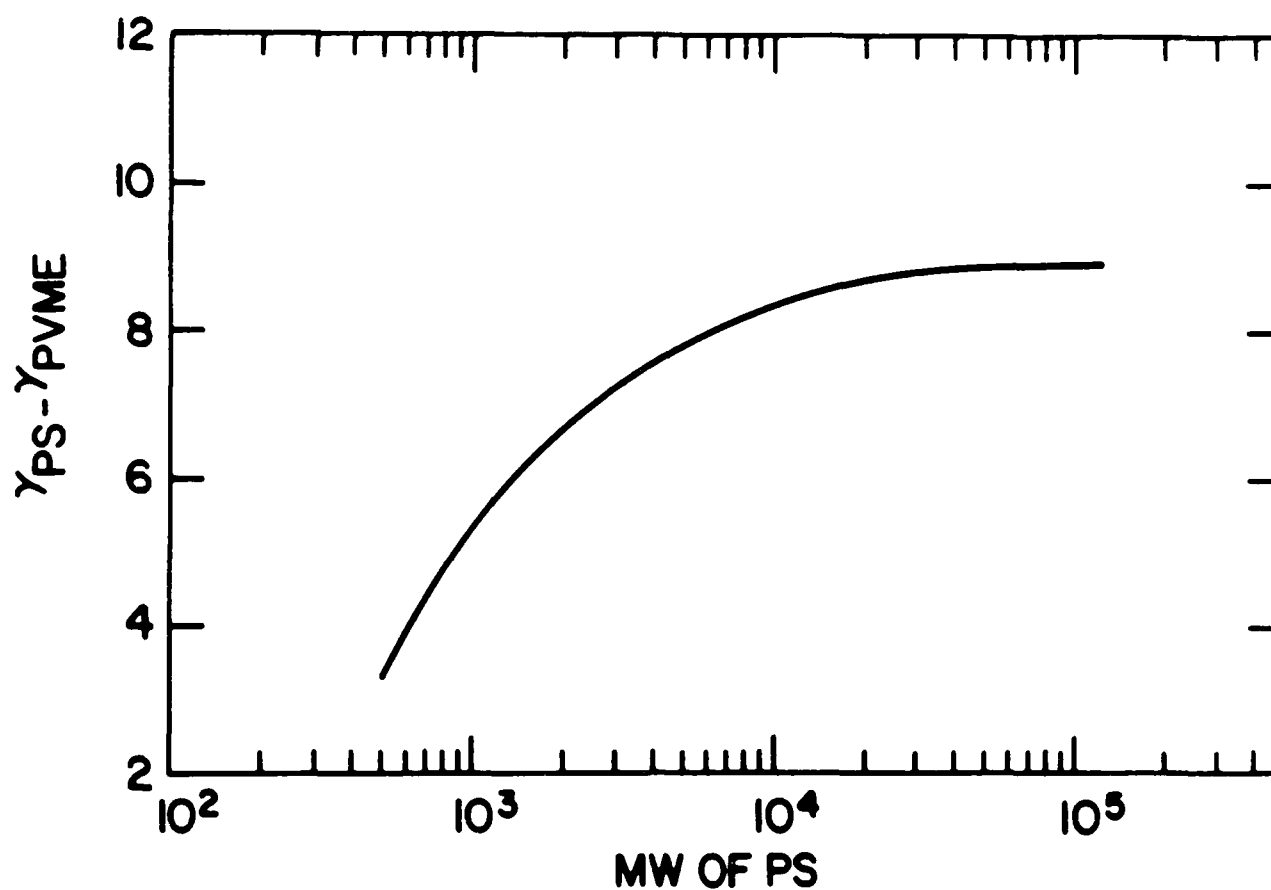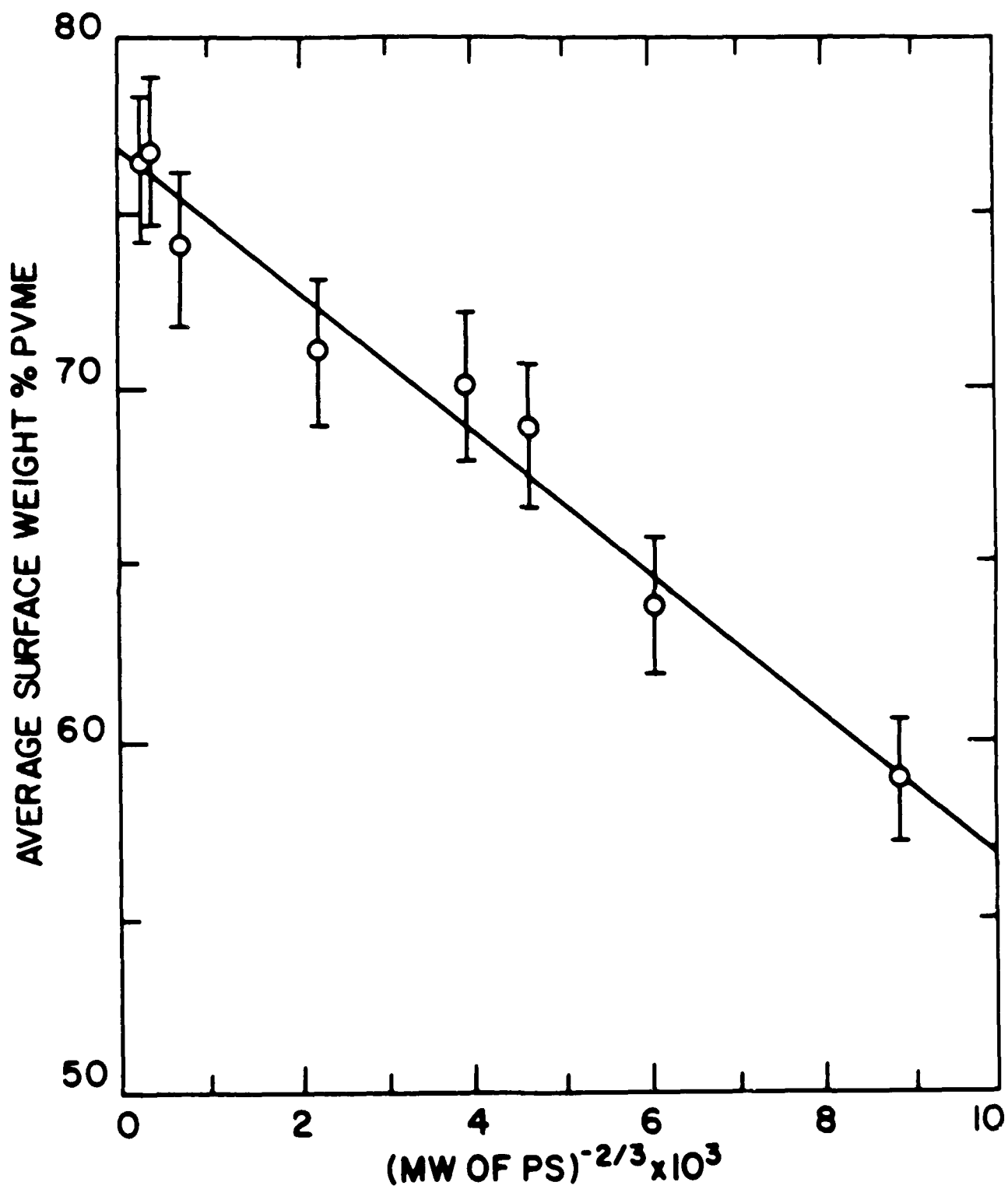
Fig. 12

Fig. 13

Fig 14

Fig. 15

END
DATE
FILMED
5-88
DTIC